

LA-UR-08-7681

Approved for public release;
distribution is unlimited.

Title: Processing and Characterization of Nanostructured
Cu-Carbon Nanotube Composites

Author(s): H. Li, A. Misra, Y.T. Zhu, Z. Horita, C.C. Koch, T.G.
Holesinger

Intended for: Composites Science and Technology



Los Alamos National Laboratory, an affirmative action/equal opportunity employer, is operated by the Los Alamos National Security, LLC for the National Nuclear Security Administration of the U.S. Department of Energy under contract DE-AC52-06NA25396. By acceptance of this article, the publisher recognizes that the U.S. Government retains a nonexclusive, royalty-free license to publish or reproduce the published form of this contribution, or to allow others to do so, for U.S. Government purposes. Los Alamos National Laboratory requests that the publisher identify this article as work performed under the auspices of the U.S. Department of Energy. Los Alamos National Laboratory strongly supports academic freedom and a researcher's right to publish; as an institution, however, the Laboratory does not endorse the viewpoint of a publication or guarantee its technical correctness.

Processing and Characterization of Nanostructured Cu-Carbon Nanotube Composites

Hongqi Li^{a*}, Amit Misra^a, Yuntian Zhu^b, Zenji Horita^c, Carl C. Koch^b, Terry G. Holesinger^d

^aCenter for Integrated Nanotechnologies, Los Alamos National Laboratory, Los Alamos, NM
87545 USA

^bDepartment of Materials Science and Engineering, North Carolina State University, Raleigh,
North Carolina 27695USA

^cDepartment of Materials Science and Engineering, Kyushu University, Fukuoka, 819-0395
Japan

^dSuperconductivity Technology Center, Los Alamos National Laboratory, Los Alamos, NM
87545 USA

*Corresponding author. E-mail address: hqli@lanl.gov

Carbon nanotube (CNT) reinforced nanostructured Cu matrix composite with a grain size less than 25nm has been successfully fabricated via a combination of ball milling and high-pressure torsion. CNTs were found to be homogeneously dispersed into the metal matrix, leading to grain refinement with a narrow grain size distribution and significant increase in hardness.

Keywords: A. Nanostructures; A. Metal-matrix composite; A. Carbon nanotubes; B. Strength

1. Introduction

Over the past two decades, carbon nanotubes (CNTs) reinforced composites have sparked intense scientific and technological interests, primarily motivated by the fact that CNTs have an extraordinary structure, and, more importantly, possess attractive properties and promising application perspectives. For example, CNTs have been found to exhibit good ductility, super-high strength and elastic modulus [1-5], which exceed those of many conventional materials. Furthermore, CNTs also own a unique set of attributes including lightweight, high aspect ratio and excellent thermal stability [5]. As a result, a combination of these exceptional properties makes CNTs an ideal reinforcement for achieving optimized properties and improved performance in composites. Different CNT-reinforced composites have been successfully synthesized. The literature data show a significant strengthening effect by adding CNTs in polymer matrices [6-8]. In addition, an improvement in toughness has also been obtained in the case of ceramic-CNT composites [9,10]. It is worth mentioning that the past research efforts mainly focused on the polymer/ceramic-based CNT composites, and studies on metal-CNT composites, especially nanostructured (<100nm) metal-CNT composites, are relatively limited. This is probably due to the difficulty in dispersing CNTs homogeneously in metallic matrices. However, research interest in the CNT-metallic matrix composites has been growing remarkably recently [11-16]. Available results demonstrate that an addition of CNTs into metallic matrices can improve hardness/strength and decrease wear loss [11-18]. Moreover, it was reported that the strength has a strong dependence on the amount of CNTs added [13,16-19]. In most cases, the grain sizes of metal-CNT composites were not specifically mentioned in the literature. Nevertheless, it is suggested that these composites should have a large grain size since their fabrication processes involved high temperature sintering [12-19] and the nanostructure is

usually not thermally stable [20]. On the other hand, high temperatures may damage the unique structure of CNTs and cause reaction between metallic matrices and CNTs [21]. As a result, detailed investigations on nanostructured metal-CNT composites have not been well conducted so far [11,22]. In the present study, nanostructured Cu-CNT composites were fabricated using a combination of ball milling, powder consolidation and high pressure torsion at room temperature, and microstructures and mechanical properties were characterized.

2. Experimental

Cu powders with particle sizes in the range of 0.5-1.5 μ m (sealed in argon) and multi-wall CNTs were used in the current study. The powder loading and high-energy ball milling were performed in an argon protected environment at room temperature. The mass ratio of ball to powder is 10:1, and the milling time is up to 5 hours. For the purpose of comparison, pure Cu and Cu-CNT composites (1wt.% CNT) were made under the same condition. The ball-milled powders were isostatically compacted into 10mm diameter discs at a pressure of about 500MPa in air at room temperature. Finally, the compacted discs were consolidated using high-pressure torsion (HPT) under 6GPa for 5 revolutions at room temperature. The microstructure characterizations were carried out using scanning electron microscopy (SEM), transmission electron microscopy (TEM), and x-ray diffraction analysis. Microhardness was measured from the center to the edge of the HPT consolidated discs. At each point, at least six measurements were conducted.

3. Results and discussion

Figure 1 presents the x-ray diffraction (XRD) pattern (CuK α radiation) and TEM characterizations of carbon nanotubes used in this study. It is clear that the diffraction pattern

exhibited a feature of hexagonal graphite, and the outside diameter of CNTs is less than 10nm. Furthermore, XRD and TEM results suggest that the purity of CNTs is good since no impurity peaks were observed in the XRD pattern and there are not a significant number of catalytic particles found during TEM investigations. The inset in Figure 1(b) is a high resolution TEM (HRTEM) image showing a multi-wall characteristic of CNTs.

Figure 2 shows the morphology of ball-milled Cu powders with and without CNTs. In general, the particle size increased remarkably from an initial size of 0.5-1.5 μm to 10-50 μm after 5 hours of ball milling. Some particles have a very smooth flat surface and reached a size of over 200 μm . Figures 2(a) and (b) illustrate that there are no significant differences in the particle morphology for samples with and without CNTs. At high magnification, a comparison between Figures 2(c) and (d) indicates that surfaces of the Cu-CNT particles are rougher and there are more small flakes on the surfaces of large particles. During mechanical alloying, the Cu powders are first flattened and fractured due to the impact of balls and then form large particles because of the cold-welding process. In other words, there exists a competition between work hardening and fracturing (decreasing particle size) and cold welding (increasing particle size). A recent investigation shows that Al-CNT (~7vol.%) particle size first increased and then began to decrease after 6 hours of ball milling [23]. Therefore, it is possible that for the Cu-CNT sample, small flakes started to form after 5 hours of ball milling. In addition, a close examination at higher magnification discloses that CNTs were not observed on the surface of Cu-CNT particles, which implies that CNTs have been incorporated into Cu matrix during the cold welding process. The repetition of powder flattening, breaking, and cold-welding during ball milling leads to a homogeneous dispersion of CNTs into Cu matrix.

The detailed microstructure analysis for the HPT processed samples with and without CNTs was conducted by TEM, as presented in Figure 3. Figures 3(a)-(d) demonstrate that both materials have a nanocrystalline microstructure and grains are equiaxed. The average grain size is about 22nm and 29nm for Cu-CNT composite and pure Cu, respectively. The grain size distribution of Cu-CNT nanocomposite is apparently tighter than that of pure Cu, as seen in Figures 3(e) and (f). It is known that the principle of producing nanostructures by HPT is to form subgrain boundaries via dislocation accumulation and rearrangements under severe torsional deformation. These subgrain boundaries then develop into high-angle grain boundaries, resulting in grain refinement. With the presence of CNTs, the dislocation motion could be blocked at CNT-Cu interfaces. That is, the dislocation accumulation would be enhanced by CNTs. Consequently, an addition of CNTs leads to a further decrease in grain size and grain size distribution. Some grains in the Cu-CNT composite are smaller than 10nm, as seen in Figure 4(a). Figure 4(b) displays a high resolution TEM picture showing a CNT embedded in the Cu matrix. The CNT's interlayer spacing of about 0.35nm is consistent with measurements from Figure 1. In addition, it is worth mentioning that during TEM observations, CNTs were found to exist inside nanocrystalline grains, which is critical to obtaining improved performance in the CNT-reinforced composites.

Figure 5 shows the x-ray diffraction patterns of HPT fabricated Cu and Cu-CNT composites, and the normalized intensities are summarized in Table 1. No chemical reaction between CNTs and copper matrix is discerned from XRD patterns. Diffraction peaks corresponding to cupric oxide were clearly detected in the as-compacted samples but not in the HPT fabricated samples. The oxidation probably occurred during the processes of both ball milling and powder compaction. The powder compaction was carried out in air. During HPT processing, the oxide layer on the Cu

powders was fragmented and dispersed into metal matrix by severe plastic deformation. The disappearance of oxide peak after HPT could also be caused by the dissolution of oxides into the Cu matrix. It has been reported that severe plastic deformation could dissolve second phases [24]. Furthermore, the XRD data show that after HPT processing, a strong (111) texture was developed. Nevertheless, an addition of CNTs did not affect the texture intensity.

The nanoindentation measured hardness as a function of distance from the disc center is plotted in Figure 6(a) for nanostructured Cu and Cu-CNT composite. It is obvious that for both samples microhardness does not change significantly with the measurement location, which indicates that the microstructure is uniform. This is in contrast with the reported dependence of hardness along the radius in an HPT processed Al-CNT nanocomposite disc [11]. This difference is presumably due to different approaches used for sample preparation. The Al-CNT composite was made directly from mixed Al and CNT powders by HPT. It is known that the grain refinement during HPT is not uniform along the radius of the disc [25]. In the current study, the Cu and CNT powders were first ball milled for a long time. Then the large agglomerated particles of the Cu-CNT composite powders were consolidated, and, finally, the compacted discs were processed into nanostructured Cu-CNT composites by HPT. Therefore, prior to HPT processing, the grains may already be refined by ball milling [26], which led to a much more uniform microstructure. Figure 6(b) presents the strength change with grain size. It has been shown that there is a significant scattering in the hardness values for small grained Cu made by different methods [27]. For the purpose of a reliable comparison, all the materials selected in Figure 6(b) were made by the same philosophy of severe plastic deformation [25,27]. Compared with the reported Cu data [27], the current Cu has the highest hardness value at a grain size of around 25nm. The primary

reason is probably related to the unique microstructure made by severe plastic deformation [27]. The oxide dispersed in matrix may also contribute to the strengthening effect. However, it is apparent that the current nanostructured Cu follows the Hall-Petch relation, and the ultrafine-grained Cu samples included in Figure 6(b) are produced directly from bulk Cu by severe plastic deformation, which suggests that the contribution of oxide to strength may not be significant. More importantly, in Figure 6(b), the strength of Cu-CNT nanocomposite is obviously higher than the Hall-Petch extrapolation for pure Cu. It is disclosed that with CNTs, an increase of about 640MPa in hardness was obtained. Such enhancement in strength originates from two aspects. One is grain refinement, and the other is due to an addition of CNTs. Similar phenomenon has also been observed in the large-grained Cu-CNT and Co-CNT composites [12,28]. Moreover, calculations find that in the current study the contribution to strength reinforcement from CNTs is larger than that from grain refinement. For example, based on the Hall-Petch plot for Cu, the increase in hardness from grain refinement is approximately 280MPa, and the addition of CNTs results in an increase in hardness of about 360MPa.

4. Summary

Nanostructured Cu-CNT composite and pure Cu with a grain size of about 22nm and 29nm, respectively, were produced using a combination of ball milling, powder consolidation and high pressure torsion. Their microstructure and hardness were characterized by x-ray diffraction, scanning electron microscopy, high resolution transmission electron microscopy and nanoindentation. The results show that the addition of CNTs did not affect the particle size of ball-milled powders and texture intensity of HPT processed nanostructures. However, the addition of 1wt.% CNTs can cause further grain refinement and helps in decreasing the grain size

distribution. In addition to the strengthening by grain refinement, the introduction of CNTs also leads to a large increase in strength. A detailed microstructure analysis reveals that the CNTs were incorporated and embedded into Cu matrix. The x-ray, nanoindentation and TEM results all indicate that the dispersion of CNTs in Cu matrix is homogeneous. These findings suggest that high quality nanostructured metal-CNT composites can be successfully fabricated at room temperature, and the addition of CNTs can improve the performance of these nanostructures.

Acknowledgements

The authors acknowledge support from a LANL Director's post-doctoral fellowship (Li) and DOE, Office of Science, Office of Basic Energy Sciences. ZH appreciates the support of Kyushu University P&P program.

References

- [1] Treacy MMJ, Ebbesen TW, Gibson JM. Exceptionally high Young's modulus observed for individual carbon nanotubes. *Nature* 1996;381:678-680.
- [2] Wong EW, Sheehan PE, Lieber CM. Nanobeam Mechanics: Elasticity, Strength, and Toughness of Nanorods and Nanotubes. *Science* 1997;271:1971-1975.
- [3] Demczyk BG, Wang YM, Cumings J, Hetman M, Han W, Zettl A, Ritchie RO. Direct mechanical measurement of the tensile strength and elastic modulus of multiwalled carbon nanotubes. *Mater Sci Eng A* 2002;334:173-178.
- [4] Zhao QZ, Nardelli MB, Bernholc J. Ultimate strength of carbon nanotubes: a theoretical study. *Phys Rev B* 2002;65:144105.
- [5] Ajayan PM. Nanotubes from carbon. *Chem Rev* 1999;99:1787-1800.
- [6] Mamedov AA, Kotov NA, Prato M, Guldi DM, Wickstedt JP, Hirsch A. Molecular design of strong single-wall carbon nanotube/polyelectrolyte multilayer composites. *Nat Mater* 2002;1:190-194.
- [7] Coleman JN, Khan U, Gun'ko YK. Mechanical reinforcement of polymers using carbon nanotubes. *Adv Mater* 2006;18:689-706.
- [8] Thostenson ET, Ren ZF, Chou TW. Advances in the science and technology of carbon nanotubes and their composites: a review. *Compos Sci Technol* 2001;61:1899-1912.
- [9] An LN, Xu WX, Rajagopalan S, Wang CM, Wang H, Fan Y, Zhang LG, Jiang DP, Kapat J, Chow L, Guo BH, Liang J, Vaidyanathan R. Carbon-nanotube-reinforced polymer-derived ceramic composites. *Adv Mater* 2004;16:2036-2040.

- [10] Pasupuleti S, Peddetti R, Santhanam S, Jen KP, Wing ZN, Hecht M, Halloran JP. Toughening behavior in a carbon nanotube reinforced silicon nitride composite. *Mater Sci Eng A* 2008;491:224-229.
- [11] Tokunaga T, Kaneko K, Horita Z. Production of aluminum-matrix carbon nanotube composite using high pressure torsion. *Mater Sci Eng A* 2008;490:300-304.
- [12] Kim KT, Eckert J, Menzel SB, Gemming T, Hong SH. Grain refinement assisted strengthening of carbon nanotube reinforced copper matrix nanocomposites. *Appl Phys Lett* 2008;92:121901.
- [13] Cha SI, Kim KT, Arshad SN, Mo CB, Hong SH. Extraordinary strengthening effect of carbon nanotubes in metal-matrix nanocomposites processed by molecular-level mixing. *Adv Mater* 2005;17:1377-1381.
- [14] He C, Zhao N, Shi C, Du X, Li J, Li H, Cui Q. An approach to obtaining homogeneously dispersed carbon nanotubes in Al powders for preparing reinforced Al-matrix composites. *Adv Mater* 2007;19:1128-1132.
- [15] George R, Kashyap KT, Rahul R, Yamdagni S. Strengthening in carbon nanotube/aluminum (CNT/Al) composites. *Scr Mater* 2005;53:1159-1163.
- [16] Deng CF, Wang DZ, Zhang XX, Li AB. Processing and properties of carbon nanotubes reinforced aluminum composites. *Mater Sci Eng A* 2007;444:138-145.
- [17] Kim KT, Cha SI, Hong SH. Harness and wear resistance of carbon nanotube reinforced Cu matrix nanocomposites. *Mater Sci Eng A* 2007;449-451:46-50.
- [18] Dong SR, Tu JP, Zhang XB. An investigation of the sliding wear behavior of Cu-matrix composite reinforced by carbon nanotube. *Mater Sci Eng A* 2001;313:83-87.

- [19] Kim KT, Cha SI, Hong SH, Hong SH. Microstructure and tensile behavior of carbon nanotube reinforced Cu matrix nanocomposites. *Mater Sci Eng A* 2006;430:27-33.
- [20] Li HQ, Ebrahimi F. An investigation of thermal stability and microhardness of electrodeposited nanocrystalline nickel-21% iron alloys. 2003;51: 3905-3913.
- [21] Ci L, Ryu Z, Jin-Phillipp NY, Rühle Manfred. Investigation of the interfacial reaction between multi-walled carbon nanotubes and aluminum. *Acta Mater* 2006;54:5367-5375.
- [22] Dai PQ, Xu WC, Huang QY. Mechanical properties and microstructure of nanocrystalline nickel-carbon nanotube composites produced by electrodeposition. *Mater Sci Eng A* 2008;483-484:172-174.
- [23] Morsi K, Esawi A. Effect of mechanical alloying time and carbon nanotube (CNT) content on the evolution of aluminum (Al)-CNT composite powders. *J Mater Sci* 2007;42:4954-4959.
- [24] Zhao YH, Liao XZ, Cheng, S, Ma E, Zhu YT. Simultaneously increasing the ductility and strength of nanostructured alloys. *Adv Mater* 2006;18:2280-2283.
- [25] Jiang HG, Zhu YT, Butt DP, Alexandrov IV, Lowe TC. Microstructural evolution, microhardness and thermal stability of HPT-processed Cu. *Mater Sci Eng A* 2000;290:128-138.
- [26] Youssef KM, Scattergood RO, Murty KL, Koch CC. Ultratough nanocrystalline copper with a narrow grain size distribution. *Appl Phys Lett* 2004;85:929-931.
- [27] Chen J, Lu L, Lu K. Hardness and strain rate sensitivity of nanocrystalline Cu. *Scr Mater* 2006;54:1913-1918.
- [28] Jeong YJ, Cha SI, Kim KT, Lee KH, Mo CB, Hong SH. Synergistic strengthening effect of ultrafine-grained metals reinforced with carbon nanotubes. *Small* 2007;3:840-844.

Table 1. Summary of texture intensity of HPT processed Cu and Cu-CNT composite.

FCC peaks	111	200	220	311	222
Standard intensity (Cu)	100	46	20	17	5
Cu	100	4	3	3	4
Cu-CNT	100	6	4	4	5

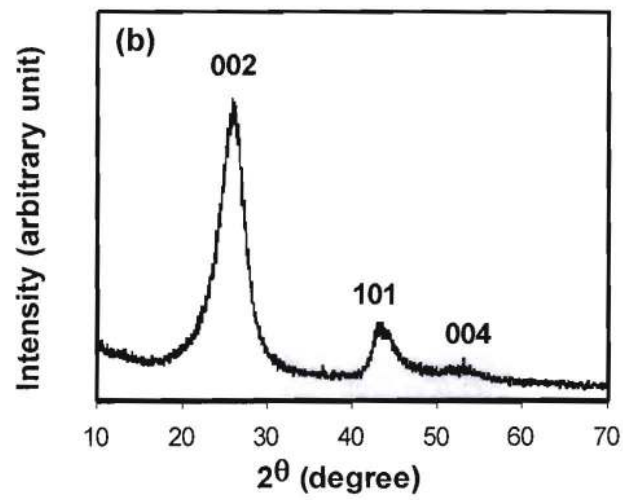
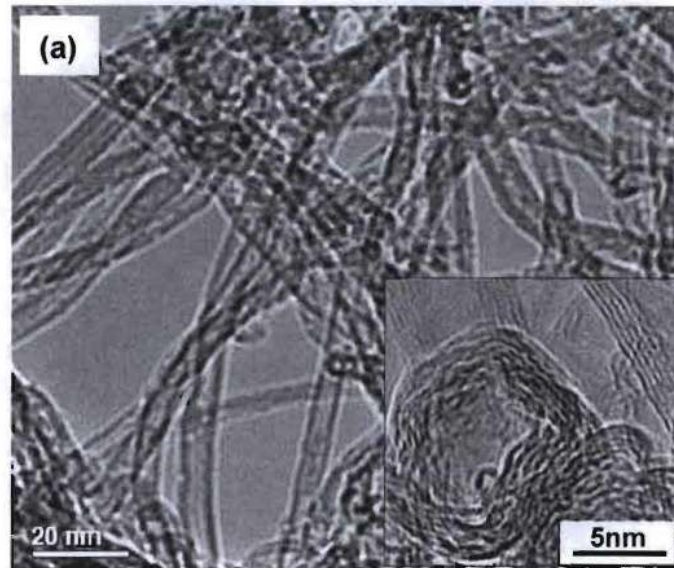


Figure 1. Microstructural characterization of as-received multi-wall carbon nanotubes. (a) TEM image and (b) x-ray diffraction pattern. The insert in (a) is a HRTEM picture.

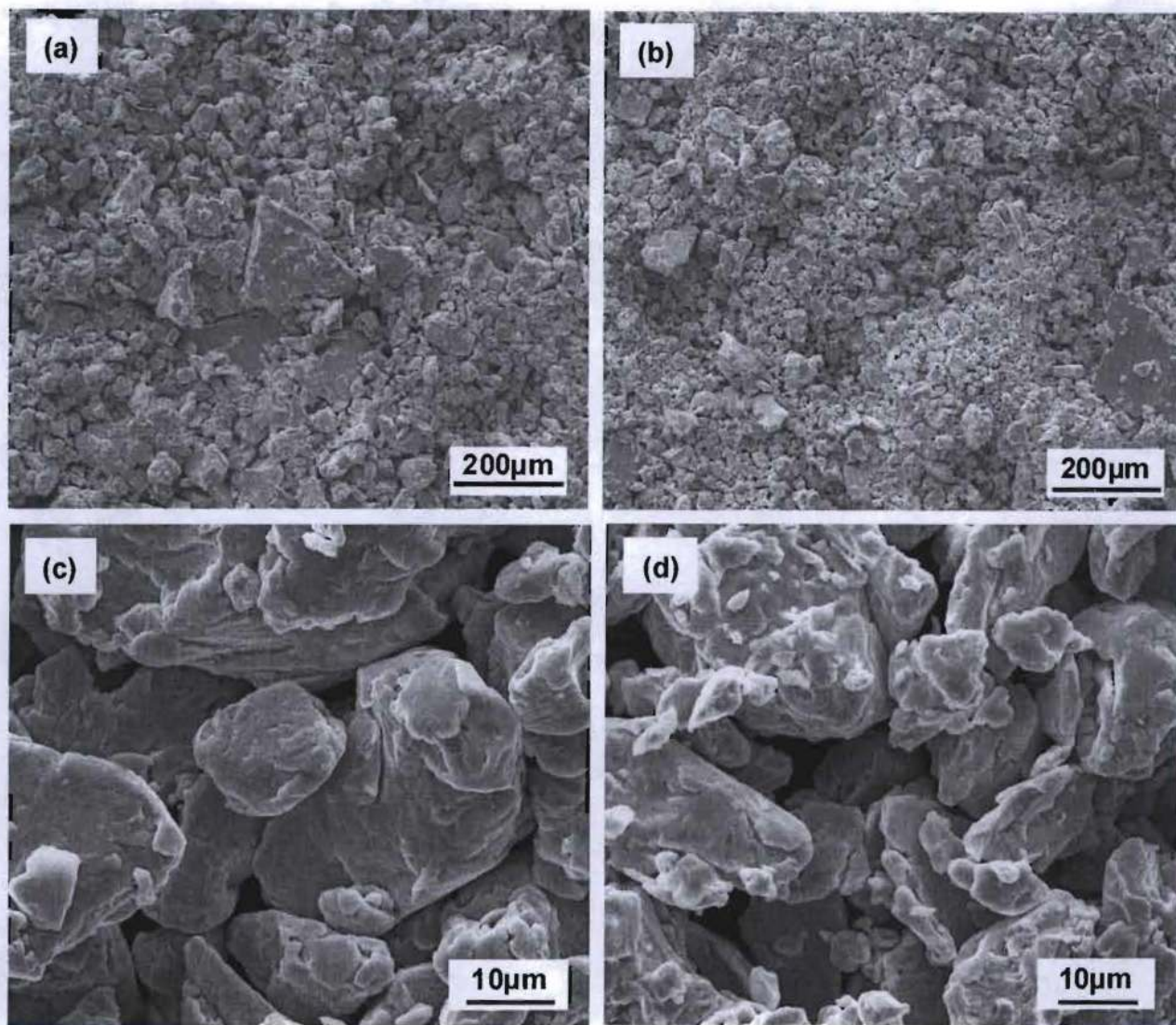


Figure 2. SEM micrographs of ball-milled Cu and Cu-CNT particles. (a) and (c) pure Cu, (b) and (d) Cu-CNT composite.

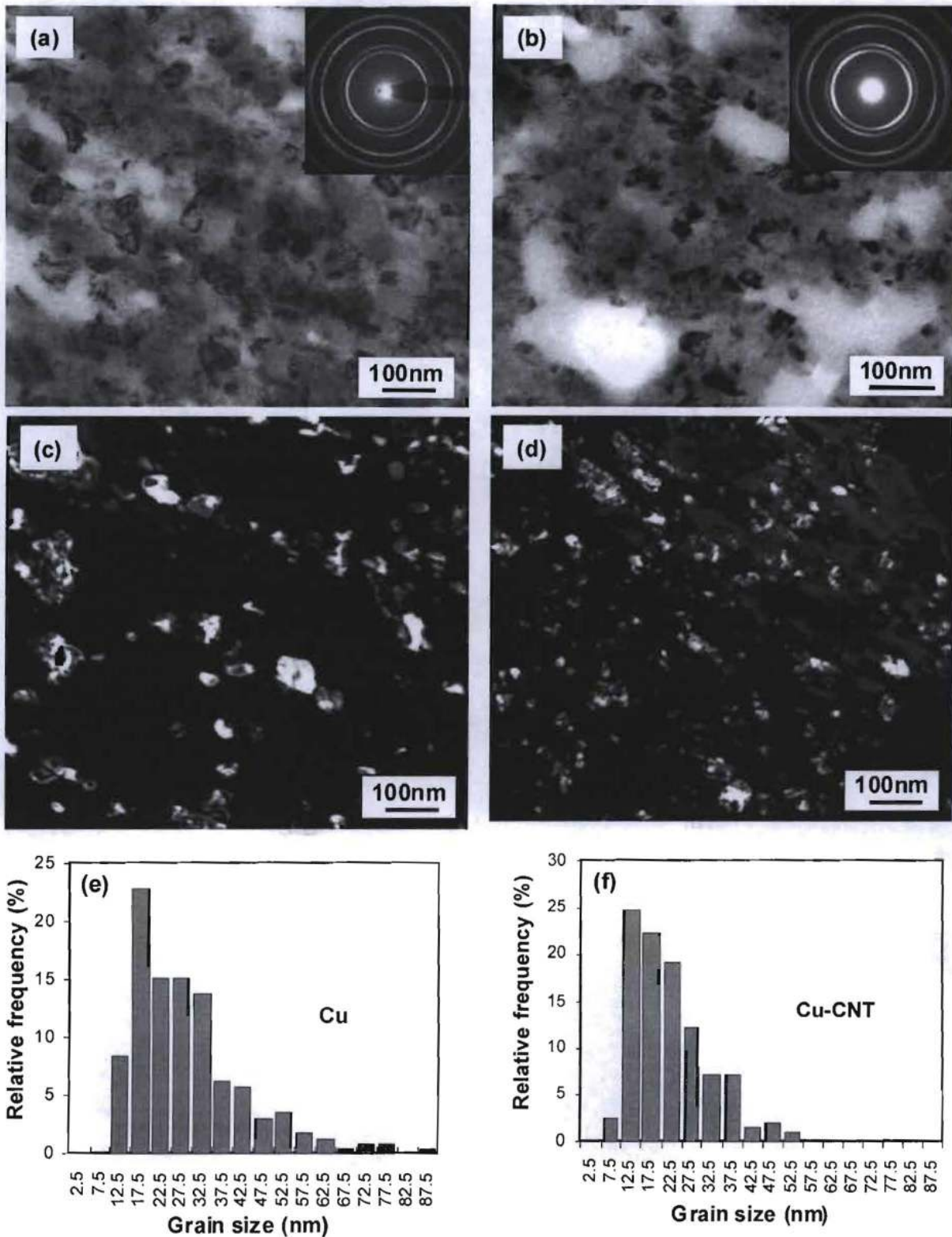


Figure 3. Bright and dark filed TEM micrographs and grain size distributions of nanostructured Cu and Cu-CNT composite. (a), (c) and (e) pure Cu; (b), (d) and (f) Cu-CNT composite.

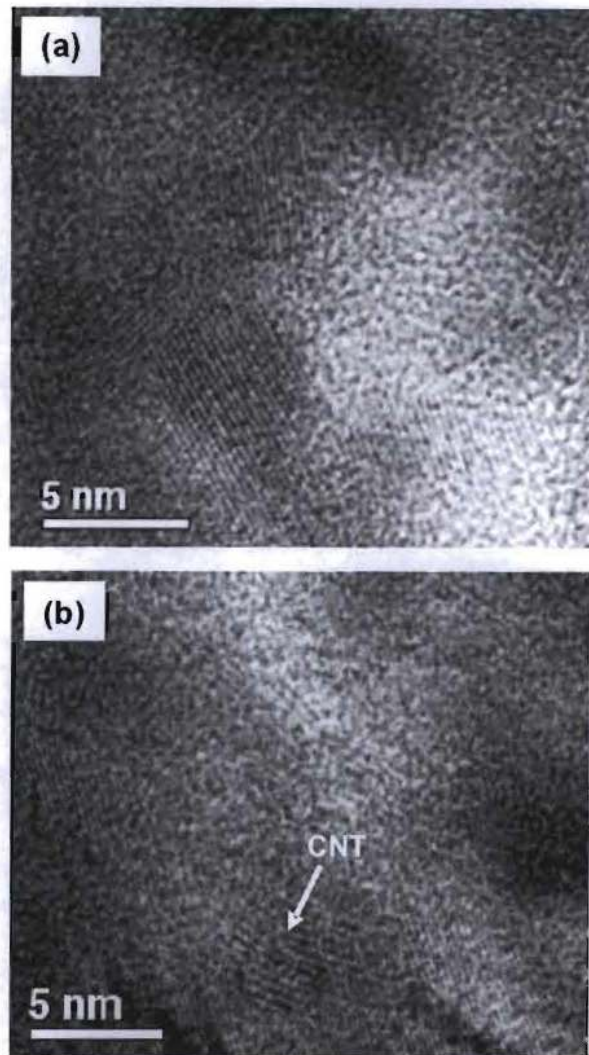


Figure 4. High resolution TEM analysis of Cu-CNT nanocomposite. (a) nanocrystalline structure of Cu matrix and (b) CNTs embedded in the Cu matrix.

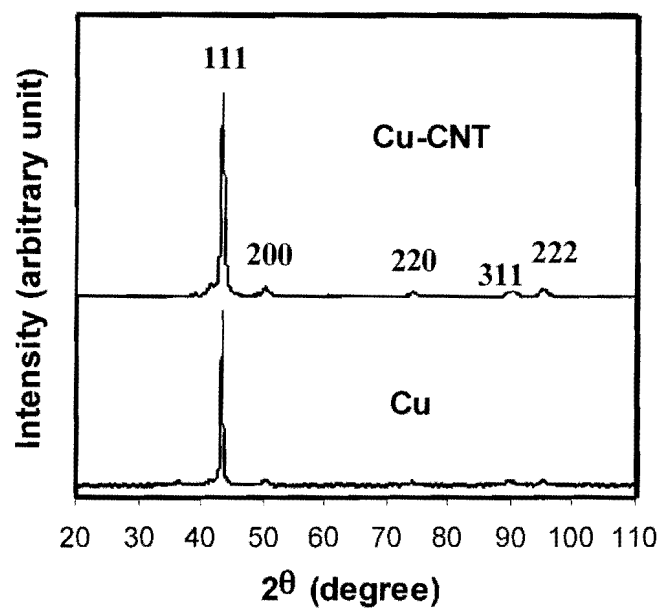


Figure 5. X-ray diffraction patterns of HPT processed nanostructured Cu and Cu-CNT composite.

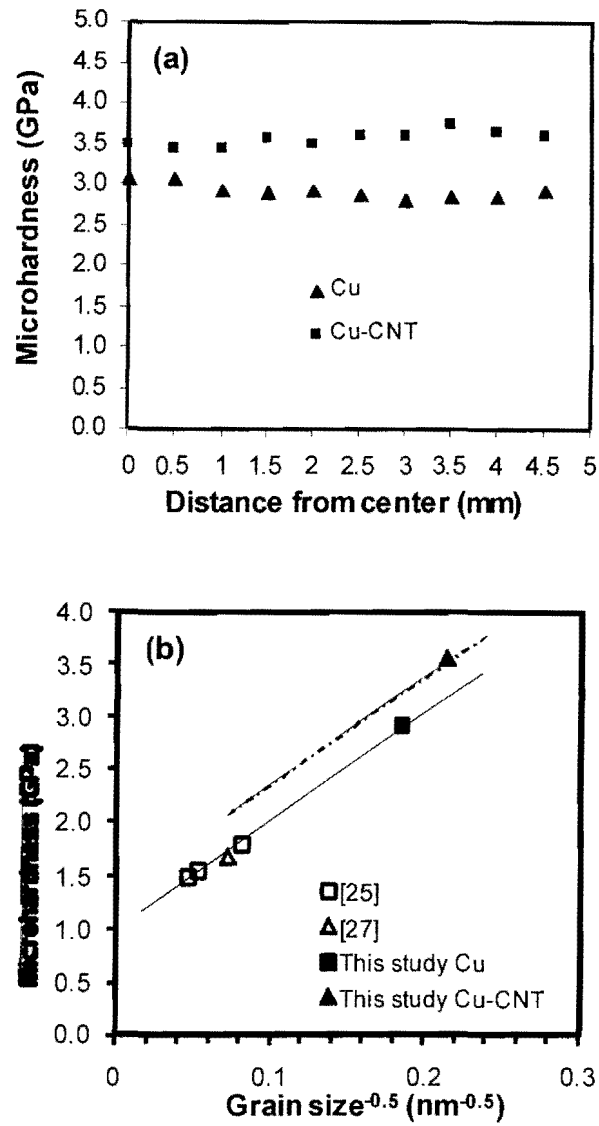


Figure 6. Flow stress as a function of distance from disc center (a) and grain size (b) for HPT processed Cu and Cu-CNT nanocomposite. In (b), the solid line is the Hall-Petch plot for pure Cu, and the dotted line is drawn as a guide to eye.